Molecular Pharmacology Fast Forward. Published on May 23, 2012 as doi: 10.1124/mol.112.078006
This article has not been copyedited and formatted. The final version may differ from this version.

TITLE PAGE

Vm24, a natural immunosuppressant peptide potently and selectively blocks Kv1.3 potassium channels of human T cells

Zoltan Varga, Georgina Gurrola-Briones, Ferenc Papp', Ricardo C. Rodríguez de la Vega, Gustavo Pedraza-Alva, Rajeev B. Tajhya, Rezso Gaspar, Luis Cardenas, Yvonne Rosenstein, Christine Beeton, Lourival D. Possani, Gyorgy Panyi

Department of Biophysics and Cell Biology, Research Center for Molecular Medicine, University of Debrecen, Debrecen, Hungary, 4032: Z.V., F.P, R.G., G.P

Departamento de Medicina Molecular y Bioprocesos, Instituto de Biotecnologia, Universidad Nacional Autónoma de México, Cuernavaca, Mexico 62210: G.G-B, G.P-A, Y.R., L.D.P.

Ecologie, Systématique et Evolution, Université Paris-Sud, F-91405, Orsay cedex, France; UMR 8079, CNRS, F-91405, Orsay cedex, France: R.C.R.V.

Departamento de Biología Molecular de Plantas, Instituto de Biotecnologia, Universidad Nacional Autónoma de México, Cuernavaca, Mexico 62210: L.C.

Department of Molecular Physiology and Biophysics, Baylor College of Medicine, One Baylor Plaza, Houston, Texas, 77030: R.B.T, C.B.

Molecular Pharmacology Fast Forward. Published on May 23, 2012 as DOI: 10.1124/mol.112.078006
This article has not been copyedited and formatted. The final version may differ from this version.

RUNNING TITLE PAGE

Running title: An immunosuppressant peptide toxin from scorpion venom

Corresponding author:
Gyorgy Panyi
Department of Biophysics and Cell Biology, Medical and Health Science Center, University of Debrecen, Nagyerdei krt. 98., Debrecen 4032, Hungary
Tel/Fax: +36 52 412 623
e-mail: panyi@med.unideb.hu

Number of text pages: 36
Number of tables: 0
Number of figures: 7
Number of references: 43
Number of words in Abstract: 114
Number of words in Introduction: 748
Number of words in Discussion: 1491

Nonstandard abbreviations used in the text:

CFSE: Carboxyfluorescein succinimidyl ester
CRAC: Ca^{2+}-release activated Ca^{2+} channel
FACS: Fluorescence activated cell sorter
Kv1.3: voltage-gated K^+ channel, Shaker-related subfamily
KCa3.1: intermediate conductance Ca^{2+}-activated K^+ channel
PBMC: Peripheral Blood Mononuclear Cell
RCF: remaining current fraction
T_{EM}: effector memory T cell

Molecular Pharmacology Fast Forward. Published on May 23, 2012 as DOI: 10.1124/mol.112.078006
This article has not been copyedited and formatted. The final version may differ from this version.

ABSTRACT

The blockage of Kv1.3 K^+ channels of T cells is a promising therapeutic approach for the treatment of autoimmune diseases such as multiple sclerosis or type I diabetes. Vm24 (α-KTx 23.1) is a novel 36 residue-long Kv1.3 specific peptide isolated from the venom of the scorpion *Vaejovis mexicanus smithi*. Vm24 inhibits Kv1.3 channels of human lymphocytes with high affinity (K_d of 2.9 pM) and exhibits >1500-fold selectivity over other ion channels assayed. It inhibits the proliferation and Ca^{2+} signaling of human T cells *in vitro* and reduces delayed-type hypersensitivity reaction in rats *in vivo*. Our results indicate that Vm24 has exceptional pharmacological properties that make it an excellent candidate to treat certain autoimmune diseases.

Molecular Pharmacology Fast Forward. Published on May 23, 2012 as DOI: 10.1124/mol.112.078006
This article has not been copyedited and formatted. The final version may differ from this version.

INTRODUCTION

Autoimmune diseases are characterized by the generation of T cell clones which react to self-antigens, thereby leading to the destruction of specific tissues such as myelinated neurons in multiple sclerosis or insulin producing pancreatic β cells in type-I diabetes mellitus (Beeton et al., 2006). In these diseases the specific inhibition of the proliferation of autoreactive T cells mediating tissue damage (effector memory T cells, T_{EM}) is desirable (Wulff et al., 2003).

A rise in the cytosolic free Ca^{2+} concentration ($[Ca^{2+}]_i$) is a key signal leading to T cell proliferation (Lewis, 2001; Cahalan and Chandy, 2009). The membrane potential of T cells, sustained by the activity of the voltage-gated depolarization activated Kv1.3 and the Ca^{2+}-activated KCa3.1 K^+ channels, contributes to the electrochemical driving force for Ca^{2+} entry into the cells trough plasma membrane CRAC channels (Leonard et al., 1992; Lin et al., 1993). CRAC assemble upon T cell activation and subsequent intracellular Ca^{2+} store depletion with STIM1 sensing the depletion of ER Ca^{2+} and Orai1 being the pore unit of the channel (Cahalan and Chandy, 2009). The activity of the K^+ channels provides the counterbalancing cation efflux required for the maintenance of the negative membrane potential during Ca^{2+} influx. The inhibition of Kv1.3 and KCa3.1 depolarizes the membrane potential and inhibits Ca^{2+} entry, thus, leading to reduced T cell proliferation (Panyi et al., 2004; Cahalan and Chandy, 2009).

T cell subtype-specific expression of K^+ channels significantly influences the potency of K^+ channel blockers to inhibit T cell proliferation. Kv1.3 is the dominant K^+ channel of T_{EM} cells and its inhibition causes a persistent suppression of T_{EM} proliferation (Wulff et al., 2003). Other T cell subsets escape the Kv1.3 blocker-mediated inhibition of proliferation by transcriptional up-regulation of KCa3.1 (Ghanshani et al., 2000). Thus, the unique dependence of T_{EM} cells on Kv1.3 for proliferation points to high affinity Kv1.3 inhibitors as potential therapeutic

Molecular Pharmacology Fast Forward. Published on May 23, 2012 as DOI: 10.1124/mol.112.078006
This article has not been copyedited and formatted. The final version may differ from this version.

immunosuppressors (Cahalan and Chandy, 2009). To avoid unwanted side-effects mediated by the blockade of other Kv channels, a very high selectivity for Kv1.3 is compelling for a therapeutically applied blocker (Panyi et al., 2006).

Animal toxins and small molecule inhibitors have been reported to display high affinity for Kv1.3 and some of the toxins are selective for Kv1.3 over KCa3.1 (Panyi et al., 2006). These include scorpion toxins (e.g., margatoxin, noxiustoxin, and kaliotoxin) and the ShK toxin isolated from a sea anemone. However, ion channels important for neuronal and muscle excitability are also inhibited by these toxins with comparable affinities [e.g., Kv1.1 is blocked by ShK (Kalman et al., 1998), whereas Kv1.2 is inhibited by margatoxin (Koch et al., 1997)]. Several successful attempts were made to engineer toxin variants with improved selectivity for Kv1.3. In the case of OSK-1 and BmKTx, this was accomplished by introducing substitutions for natural amino acids in key positions (e.g. [K16,D20]-OSK1 (Mouhat et al., 2005) and [R11,T28,H33]-BmKTx (Han et al., 2008)) resulting in over 100-fold selectivity for Kv1.3, while maintaining (OSK-1 mutant) or increasing the affinity (BmKTx mutant) for Kv1.3. ShK mutants containing a non-natural amino acid (ShK-Dap22) or various N-terminal modifications (e.g. ShK-192 (Pennington et al., 2009)) also resulted in peptides with distinctive selectivity and affinity for Kv1.3

We describe here the exceptional pharmacological properties of Vm24, a natural peptide, identified as part of the proteomic analysis of venom collected from the Mexican scorpion *Vaejovis mexicanus smithi*. Vm24, the first member of a novel αKTx subfamily, is a 36-residue-long peptide cross-linked by eight cysteines forming a distorted Cysteine Stabilized α/β motif; (details provided in (Gurrola et al., 2012)). Although Vm24 shares structural similarities with other K^+ channel blockers (i.e., α-helix and β turns with a diad-like arrangement of K25 and Y34

Molecular Pharmacology Fast Forward. Published on May 23, 2012 as DOI: 10.1124/mol.112.078006
This article has not been copyedited and formatted. The final version may differ from this version.

(Dauplais et al., 1997)) it shows less than 50% identity to other known αKTx-peptides. In this paper we tested whether the unique primary structure of Vm24 is reflected in its pharmacological properties. Vm24 blocked Kv1.3 channels with very high affinity (Kd=2.9 pM) and with greater than 1500-fold selectivity against a panel of channels used in this study (hKv1.3 >>> hKv1.2 > hKCa3.1 > mKv1.1 >>> hKv1.4 ≈ hKv1.5 ≈ rKv2.1 ≈ hKv11.1 ≈ hKCa1.1 ≈ hKCa2.3 ≈ $hNa_V1.5$). Vm24 inhibited Ca^{2+} signaling of human T lymphocytes in concentrations that block Kv1.3 and *in vitro* T cell proliferation whilst being effective in reducing the delayed-type hypersensitivity in rats. The unique affinity and selectivity of the natural peptide for Kv1.3 makes of Vm24 an excellent candidate for Kv1.3 blockade-mediated treatment of certain autoimmune diseases, such as multiple sclerosis, rheumatoid arthritis and type-1 diabetes.

Molecular Pharmacology Fast Forward. Published on May 23, 2012 as DOI: 10.1124/mol.112.078006
This article has not been copyedited and formatted. The final version may differ from this version.

MATERIALS AND METHODS

Isolation and sequence determination of Vm24: A detailed description of the procedures of venom preparation, purification, proteomics, sequence and 3D NMR structure determination, as well as phylogenetic tree analysis and molecular modeling of the interaction of Vm24 with K^+-channels can be found in Gurrola et al. (Gurrola et al., 2012). Briefly, the soluble venom of *Vm smithi* was separated by high performance liquid chromatography (HPLC) and each one of the components were collected separately and immediately freeze-dried. The molecular mass of each sub-fraction was evaluated by mass spectrometry analysis using equipment and procedures described earlier (Batista et al., 2007). Fractions containing molecular weights in the range expected for K^+ channel blockers (~4000 Da) were selected for electrophysiological assays. Among these fractions was one eluting at 24 min, which was further separated, producing a homogeneous peptide, with molecular mass of 3864 Da, named Vm24. Since this component was shown to be a potent inhibitor of Kv1.3 channels, its full amino acid sequence was determined. Direct sequencing analysis was performed by automatic Edman degradation and confirmed by mass spectrometry determination. Initial sequencing results of Vm24 gave unequivocal amino acid sequence for the first 23 amino acid residues. Two peptides obtained by endopeptidase Arg-C1 cleavage allowed the identification of the sequences ranging from residues in position A18 to R29 and K30 to C36. The overlap was obtained with two additional peptides, one from a tryptic digestion which allowed the identification of residues that goes from C26 to K32, and a confirmatory peptide obtained from Lys-C digestion that corresponded to sequences from C33 to C36 (Gurrola et al., 2012). The full sequence obtained was: AAAISCVGSPECPPKCRAQGCKNGKCMNRKCKCYYC-amide (Gurrola et al., 2012).

Molecular Pharmacology Fast Forward. Published on May 23, 2012 as DOI: 10.1124/mol.112.078006
This article has not been copyedited and formatted. The final version may differ from this version.

Human T lymphocytes for patch-clamp recording: Heparinized human peripheral venous blood was obtained from healthy volunteers. Mononuclear cells were separated by Ficoll-Hypaque density gradient centrifugation. Collected cells were washed twice with Ca^{2+} and Mg^{2+} free Hank's solution containing 25 mM HEPES buffer (pH 7.4). Cells were cultured in a 5% CO_2 incubator at 37 ^{o}C in 24 well culture plates in RPMI-1640 supplements with 10% FCS (Hyclone, Logan, Utah, USA), 100 μg/ml penicillin, 100 μg/ml streptomycin and 2 mM L-glutamine at 0.5 x 10^6/ml density for 3-4 days. The culture medium also contained 6 or 8 μg/ml of phytohemagglutinin A (PHA-P, Sigma-Aldrich Kft, Hungary) to increase K^+ channel expression. T lymphocytes were selected for recording human Kv1.3 currents (hKv1.3) by incubation with mouse anti-human CD2 (Becton-Dickinson, San Jose, CA, USA) followed by selective adhesion to Petri dishes coated with goat anti-mouse IgG antibodies (Biosource, Camarilo, CA, USA), as described by Matteson and Deutsch (Matteson and Deutsch, 1984). Dishes were washed gently five times with 1 ml of normal extracellular bath medium (see below) for the patch-clamp experiments.

Human T cells for proliferation assay: The buffy coat containing mononuclear cells was resuspended in RPMI 1640 supplemented with 5% fetal calf serum (Hyclone, Logan, UT), 2 mM L-glutamine (Sigma), 50 units/mL penicillin, 50 μg/mL streptomycin and 50 mM β-mercaptoethanol before plating the cells overnight onto 100-mm Petri dishes (8×10^7 cells/plate) at 37 °C in 5% CO_2. Prior to experimentation, non-adherent cells (PBMCs) were cultured for 24 h at 37 C, 5% CO_2 in RPMI supplemented with 2% fetal calf serum.

Activation of T cells for proliferation assay: cells were stimulated with anti-CD3 (OKT3, ATCC; 100 ng/mL) and anti-CD28 (Ancell; 500 ng/mL) mAbs for 15 min at room temperature, after which a secondary anti-mouse polyclonal antibody (rabbit anti-mouse immunoglobulin,

Molecular Pharmacology Fast Forward. Published on May 23, 2012 as DOI: 10.1124/mol.112.078006
This article has not been copyedited and formatted. The final version may differ from this version.

1μg/mL) was added to crosslink primary antibodies (Fierro et al., 2006). Cells were then incubated at 37 °C 5% CO_2 for the indicated times. CD25 expression was evaluated 24 hrs after stimulation and, cell proliferation was assessed by CFSE dilution 96 hrs post-stimulation. Prior to activation, PBMCs (3-10×10^6/mL) were labeled with CFSE (0.5 μM, Molecular Probes) for 10 min at 37 °C in the dark, washed with supplemented RPMI to eliminate excess dye, and set into culture conditions as described (Muul et al., 2008). Vm24 in various concentrations was added at the onset of stimulation or 30 minutes prior to stimulation.

FACS staining and FACS analysis: Cells (1×10^6) resuspended in 100 μL of phosphate buffered saline containing 2% fetal calf serum and 1% sodium azide (FACS solution) were incubated with PE-labeled anti-CD25-PE (Caltag) and anti-CD3-TC (Caltag) for 30 min at 4°C. Cells were then washed by centrifugation at 300 g with FACS solution and fixed in 1% paraformaldehyde. Cells were acquired with a FACSort with the CELLQUEST program (Becton and Dickinson, San José, CA), and analyzed with FlowJo (TreeStar), gating on the $CD3^+$ population.

Cells for heterologous expression of ion channels: Cos-7, HEK-293, tsA-201, L929 and MEL cells were grown under standard condition as described previously (Bagdany et al., 2005; Grissmer et al., 1994; Corzo et al., 2008).

Expression of recombinant ion channels: Cos-7 cells were used to express *rat Kv2.1* (rKv2.1, kind gift from Dr. S. Korn, University of Connecticut, Storrs, USA); *human Kv1.2* (hKv1.2, pcDNA3/Hygro vector containing the full coding sequence for Kv1.2, kind gift from Dr. S. Grissmer, Ulm University, Ulm, Germany); *human Kv1.4* (hKv1.4-IR: the inactivation ball deletion mutant of Kv1.4, the kind gift from D. Fedida, University of British Columbia, Vancouver, Canada); *human KCa3.1* (hIKCa1 gene, AF033021) and *human KCa2.3 (hSKCa3 gene)* both in pEGFP-C1 vector (Wulff et al., 2001), kind gift from H. Wulff, University of

Molecular Pharmacology Fast Forward. Published on May 23, 2012 as DOI: 10.1124/mol.112.078006
This article has not been copyedited and formatted. The final version may differ from this version.

California, Davis, USA. These channel clones were transiently co-transfected with a plasmid encoding the green fluorescence protein (GFP) (except hKCa3.1 and hKCa2.3 which were in an EGPF vector) at molar ratios of 1:5 using Lipofectamine 2000, according to the manufacturer's protocol (Invitrogen, Carlsbad, CA, USA), and cultured under standard conditions. Currents were recorded 24 h after transfection. GFP positive transfectants were identified in a Nikon TE2000U fluorescence microscope and used for current recordings (>70% success rate for co-transfection).

The tsA-201 cells were used to express *hNav1.5* (a gift from R. Horn, Thomas Jefferson University, Philadelphia, USA) and *hKCa1.1* (hSlo1 gene (U11058), in pCI-neo plasmid, a gift from T. Hoshi, University of Pennsylvania, Philadelphia, USA).

L929 cells stably expressing *mKv1.1* and MEL cells stably expressing hKv1.5 channels have been described earlier (Grissmer et al., 1994) and were the kind gift of Dr. Heike Wulff (University of California, Davis, USA). *hKv11.1* **(***hERG)* channels were expressed in a stable manner in HEK-293 cells.

Electrophysiology. Whole-cell currents were measured according to standard protocols in the laboratory (Peter et al., 2001; Bagdany et al., 2005; Corzo et al., 2008) in voltage-clamped cells with Axopatch 200A and Multiclamp 700B amplifiers connected to a personal computer using Axon Digidata 1200 and 1322A data acquisition hardware, respectively (Molecular Devices Inc., Sunnyvale, CA). Series resistance compensation up to 70% was used to minimize voltage errors and achieve good voltage-clamp conditions. Cells were observed with Nikon TE2000-U or Leitz Fluovert fluorescence microscopes using bandpass filters of 455-495 nm and 515-555 nm for excitation and emission, respectively. Cells displaying strong fluorescence were selected for current recording and >70 percent of these cells displayed co-transfected current. Pipettes were

Molecular Pharmacology Fast Forward. Published on May 23, 2012 as DOI: 10.1124/mol.112.078006
This article has not been copyedited and formatted. The final version may differ from this version.

pulled from GC 150 F-15 borosilicate glass capillaries in five stages and fire-polished, resulting in electrodes having 3 to 5 MΩ resistance in the bath. For the measurement of most channels the bath solution consisted of (in mM) 145 NaCl, 5 KCl, 1 $MgCl_2$, 2.5 $CaCl_2$, 5.5 glucose, and 10 HEPES, pH 7.35, supplemented with 0.1 mg/ml bovine serum albumin (Sigma-Aldrich). For the recording of hKv11.1 (hERG) currents the bath solution contained (in mM) 140 Choline-Cl, 5 KCl, 2 $MgCl_2$, 2 $CaCl_2$, 0.1 $CdCl_2$, 20 glucose, and 10 HEPES, pH 7.35. The measured osmolarity of the external solutions was between 302 and 308 mOsm/L. The internal solution consisted of (in mM) 140 KF, 2 $MgCl_2$, 1 $CaCl_2$, 10 HEPES, and 11 EGTA, pH 7.22. For the recording of hKCa1.1 (hBK) currents the composition of the pipette filling solution was (in mM) 140 KCl, 10 EGTA, 9.69 $CaCl_2$, 5 HEPES (pH 7.2). The free Ca^{2+} concentration of this latter solution is $[Ca^{2+}]_i$ = 5 μM, which allows the recording of hKCa1.1 currents at moderate depolarizing potentials (Avdonin et al., 2003). For the recording of KCa3.1 and KCa2.3 currents the composition of the pipette filling solution was (in mM) 150 K-aspartate, 5 HEPES, 10 EGTA, 8.7 $CaCl_2$, 2 $MgCl_2$, (pH 7.2). This solution contained 1 μM free Ca^{2+} concentration to fully activate the KCa3.1 current (Grissmer et al., 1993). For the recording of Kv11.1 currents the pipette solution contained (in mM) 140 KCl, 10 EGTA, 2 $MgCl_2$, 10 HEPES (pH 7.3). The measured osmolarity of the internal solutions was approximately 295 mOsm/L. Bath perfusion around the measured cell with different test solutions was achieved using a gravity-flow perfusion system. Excess fluid was removed continuously.

For the measurement of the currents of mKv1.1, hKv1.2, hKv1.3, fast inactivation-removed hKv1.4 (Kv1.4ΔN), hKv1.5 and rKv2.1 channels voltage steps to +50 mV were applied from a holding potential of −120 mV every 15 or 30 s. For hKv11.1 (hERG) channels currents were evoked by a voltage step to +20 mV followed by a step to −40 mV during which the peak

Molecular Pharmacology Fast Forward. Published on May 23, 2012 as DOI: 10.1124/mol.112.078006
This article has not been copyedited and formatted. The final version may differ from this version.

current was measured. The holding potential was −80 mV, pulses were delivered every 30 s. For KCa1.1 channels a voltage step to +50 mV was applied, preceded by a 10-ms hyperpolarization to −120 mV from a holding potential of 0 mV. Pulses were delivered every 5 s. Currents through Ca^{2+} activated K^+ channels of T lymphocytes (hKCa3.1 or hIKCa1) were elicited by voltage ramps from -120 to +50 mV from a holding potential of −120 mV every 10s. A similar protocol was used for measuring human KCa2.3 currents except the voltage ramps were started from the holding potential of −100 mV. Currents through Nav1.5 channels were evoked by voltage steps to 0 mV from a holding potential of −120 mV every 15 s.

For data acquisition and analysis, the pClamp8/10 software package (Molecular Devices Inc., Sunnyvale, CA) was used. Generally, currents were low-pass filtered using the built in analog 4-pole Bessel filters of the amplifiers and sampled (2-50 kHz) at least twice the filter cut-off frequency. Before analysis, whole-cell current traces were corrected for ohmic leakage and digitally filtered (three-point boxcar smoothing). Each data point on the concentration-response curve represents the mean of 3-7 independent experiments, and error bars represent SEM. Data points were fitted with a two parameter Hill-equation: $RCF = K_d^n / (K_d^n + [Tx]^n)$, where RCF is the Remaining Current Fraction ($RCF = I / I_0$, where I and I_0 are the current amplitudes in the presence and absence of the toxin of given concentration, respectively), K_d is the dissociation constant, n is the Hill coefficient and [Tx] is the toxin concentration. Where indicated, K_d was estimated from RCF obtained at a single toxin concentration and using n=1 for the Hill equation.

Operational definition of equilibrium block: Due to the extremely slow blocking kinetics of the current we could not determine equilibrium block at low picomolar [Vm24] where block equilibrium would require 0.5-1 h toxin application to develop. Under these conditions the drop in the peak current from episode-to-episode was so small that an apparent saturation was

Molecular Pharmacology Fast Forward. Published on May 23, 2012 as DOI: 10.1124/mol.112.078006
This article has not been copyedited and formatted. The final version may differ from this version.

observed during data collection, although the block might not have reached its equilibrium value yet. During extended periods of toxin application, significant rundown of the whole-cell currents may happen. Moreover, rundown of the peaks could not be determined independently due to the extremely long wash-out kinetics of the peptide. These factors indicated the use of an operational definition of equilibrium block as the peak current where consecutive pulses in the presence of the toxin caused a negligible drop in the peak current (less than 2%). This means that in the RCF = I / I_0 equation I is overestimated, and thus, the K_d determined from the dose-response curve is also overestimated.

Measurement of intracellular Ca^{2+} concentration: Human peripheral T cells were loaded with 1 μM Fura2/AM (Molecular Probes) for 30 min at 37^{o}C, and plated on poly-L-Lysine coated LabTek chambers (Nunc) at 1.5×10^{6} cells/mL/chamber, in the absence or presence of 10nM Vm24 for 30 min before activation. Under a fluorescence microscope, T cells were incubated with 100 ng/mL anti-CD3 mAb and 500 ng/mL anti-CD28 mAb for 2 min prior to crosslink anti-CD3 and -CD28 mAbs with 1 μg/mL of rabbit anti-mouse IgG (RAMIG). Finally, cells were treated with 5 mM of the calcium ionophore Ionomycin. The changes in intracellular Ca^{2+} levels were analyzed with the MetaMorph/MetaFluor (Universal Imaging) software.

***In vivo* delayed type hypersensitivity (DTH) reaction.**

All animal trials were approved by the Baylor College of Medicine Institutional Animal Use and Care Committee. Female Lewis rats (9-10 weeks old) were purchased from Harlan-Sprague Dawley (Indianapolis, IN, USA) and housed under pathogen-free conditions with food and water *ad libitum*.

Active DTH was induced as described (Beeton and Chandy, 2007a) by immunizing rats against ovalbumin emulsified with complete Freund's adjuvant (Sigma, St Louis, MO, USA). Animals

Molecular Pharmacology Fast Forward. Published on May 23, 2012 as DOI: 10.1124/mol.112.078006
This article has not been copyedited and formatted. The final version may differ from this version.

were challenged 7 days later with ovalbumin in the pinna of one ear (20 μg/20 μl saline, (challenged ear)). The other ear received saline (challenge control). Rats received a single subcutaneous injection in the scruff of the neck of either vehicle (PBS + 2% rat serum) or 0.1 mg/kg Vm24 in 0.5 ml vehicle at time of challenge.

Adoptive DTH was induced as described (Beeton and Chandy, 2007b) by the intraperitoneal injection of *in vitro*-activated Ova-GFP T lymphocytes (5 million/rat; a kind gift from Dr. Flügel, University of Goettingen, Germany) in 1 ml saline. Rats were challenged in the ear and received Vm24 or vehicle 2 days later as described above.

In both DTH reactions ear thickness was measured 24 hours following the challenge using a spring-loaded micrometer (Mitutoyo, Aurora, IL, USA) with 3 digit precision. The mean of six measures at the same point were calculated and used for the statistical analysis. Specific ear swelling (Δ ear thickness) was calculated as follows: challenged ear (ovalbumin) thickness minus challenge control ear (PBS) thickness.

Molecular Pharmacology Fast Forward. Published on May 23, 2012 as DOI: 10.1124/mol.112.078006
This article has not been copyedited and formatted. The final version may differ from this version.

RESULTS

Vm24 is a high affinity blocker of Kv1.3 channels

The standard voltage protocol to evoke voltage-gated Kv1.3-mediated K^+ currents in T cells consisted of a series of 14-ms-long depolarizations to +50 mV from a holding potential of −120 mV. The time between voltage pulses was set to 15 s in order to avoid cumulative inactivation of hKv1.3 channels. Representative current traces in normal bath solution are shown in Fig. 1A (control). Under the experimental conditions detailed in Materials and Methods and in the figure legend (the lack of Ca^{2+} in the pipette-filling solution and the voltage protocol used) hKv1.3 channels are exclusively responsible for the whole-cell currents (Peter et al., 2001). Fig. 1A displays macroscopic K^+ currents through hKv1.3 channels recorded sequentially in the same cell, before (control traces) and following the addition of 1 nM Vm24 to the external solution by perfusion. The Kv1.3 current completely disappeared by the 12^{th} pulse (corresponding to 3 min) in the presence of 1 nM Vm24. Washing the perfusion chamber with toxin-free solution for several minutes resulted in no significant amount of current recovery (not shown).

The kinetics of the development of the current inhibition at 1 nM and 0.3 nM Vm24 concentrations are shown in Fig. 1B. Following the 4^{th} pulse in control solution the extracellular perfusion was switched to a toxin-containing solution and the depolarizing pulses continued every 15 s. Peak currents were determined and normalized to the peak current in control solution and plotted as a function of time. At higher toxin concentration, the kinetics of current inhibition was faster, as expected from a pseudo-first order reaction between the toxin and the channels. Remarkably, at either concentration, the toxin totally inhibited the whole-cell Kv1.3 current. Perfusing the recording chamber with toxin-free control solution resulted in a very small relief of the block within the first 8 minutes (not shown). During a 10.5-minute-period of the application

Molecular Pharmacology Fast Forward. Published on May 23, 2012 as DOI: 10.1124/mol.112.078006
This article has not been copyedited and formatted. The final version may differ from this version.

of the toxin at 3 pM concentration (Fig. 1C) the loss of the current apparently saturated at ~36% of the peak recorded in control solution. Toxin application was followed by a 30 minute washout period (arrow indicates the start of the perfusion with toxin-free solution) during which one third of the blocked current was recovered with an extremely slow kinetics (the estimated time constant for washout is τ_{out}~3800 s corresponding to an off rate of k_{off}~2.63×10^{-4} s^{-1}).

Fig. 1D shows the analysis of the kinetics of the development of the current inhibition at various Vm24 concentrations. The kinetics was characterized by fitting a single-exponential decay function to the normalized peak current-time relationships (Fig. 1B). Assuming a bimolecular reaction between the toxin and the channel, the resulting wash-in time constant ($\tau_{Vm24,in}$) is $1/(k_{on}\times[Vm24] + k_{off})$ where k_{on} and k_{off} are the molecular rate constants of toxin association to and dissociation from the channel and [Vm24] is the peptide concentration. Due to the extremely slow wash-out kinetics, and consequently the negligible value of k_{off} ($k_{off} = 1/\tau_{out}$), the off-rate of the toxin was neglected at [Vm24]≥10 pM and k_{on} was determined as the reciprocal of the wash-in time constant, i.e., $k_{on} \approx 1/\tau_{Vm24,in}$. Plotting $1/\tau_{Vm24,in}$ as a function of [Vm24] resulted in a linear relationship with $k_{on}=9.55\times10^{7}$ $M^{-1}s^{-1}$ (Fig. 1D, $r^2=0.99$, linear regression).

To prove that, similar to the action of other scorpion toxins, the inhibition of the current by Vm24 is a consequence of a block of Kv1.3 channels, we designed competition experiments between Vm24 and charybdotoxin (ChTx). ChTx is a well-characterized blocker of several K^+ channels known to occlude the pore by binding in the extracellular mouth of the channels (Goldstein and Miller, 1993). We determined $\tau_{Vm24,in}$ for 0.3 nM Vm24 in the absence of ChTx (Fig 1) and in the presence of various concentrations of ChTx following the equilibration of the block of the Kv1.3 channels (Fig. 2). We chose 0.3 nM Vm24 for the competition experiments

Molecular Pharmacology Fast Forward. Published on May 23, 2012 as DOI: 10.1124/mol.112.078006
This article has not been copyedited and formatted. The final version may differ from this version.

since it causes complete current inhibition with a kinetics that can be accurately measured considering the minimum 15 s interval between successive current recordings. Fig. 2A shows a representative experiment when the current was blocked by 0.3 nM ChTx, and thereafter the perfusion was switched to an extracellular solution containing 0.3 nM Vm24 plus 0.3 nM ChTx. If the toxins compete for the same binding sites, then a slower blocking rate by Vm24 is expected in the presence of ChTx, since only a fraction of the channels, determined by the ChTx concentration, is available for block by Vm24. Fig. 2B shows normalized peak currents recorded in different cells in the presence of only 0.3 nM Vm24, or in the presence of both toxins simultaneously following the equilibration of block by 0.3 nM or 2.5 nM ChTx. The reduction of the peak currents followed an exponential decay in all cases and the block rate was determined as $1/\tau_{in,Vm24}$ (see above). $1/\tau_{in,Vm24}$ was plotted in Fig. 2C as a function of channels not blocked by ChTx, the latter term represents the remaining current fraction (RCF) in the sole presence ChTx (RCF=I/I_0 where I and I_0 are the peak currents measured in the presence of the toxin after equilibration of the block and in the absence of the toxin, respectively.) Fig. 2C shows that $1/\tau_{in,Vm24}$ is directly proportional to RCF ($r^2 = 0.967$) as expected for two toxins competing for the same binding site.

When determining the dose-dependence of current inhibition by Vm24, accurate measurement of equilibrium block at low picomolar concentrations required special analysis due to the very slow blocking kinetics. Using the method detailed in the Materials and Methods RCF was determined and plotted as a function of the toxin concentration. The dose-response relationship was obtained by fitting the data points with the Hill-equation (Fig. 3, see Figure legend), which yielded a dissociation constant of $K_d = 2.9$ pM and a Hill coefficient of n~1.

Molecular Pharmacology Fast Forward. Published on May 23, 2012 as DOI: 10.1124/mol.112.078006
This article has not been copyedited and formatted. The final version may differ from this version.

Vm24 exhibits more than 1500-fold selectivity for Kv1.3 over KCa3.1, Kv1.1 and Kv1.2 and does not inhibit a wide range of other channels.

For a peptide to be an efficient immunosuppressant it needs to be selective for Kv1.3 over other biologically relevant channels. As mentioned in the introduction, hKCa3.1 is notable in this respect as it is also expressed endogenously in T cells (Grissmer et al., 1993) and its expression level varies among different T cell subsets (Wulff et al., 2003). The potency of Vm24 to inhibit hKCa3.1 channels was assayed on channels expressed heterologously in COS-7 cells. Although human peripheral blood T cells also express hKCa3.1 we chose to use the recombinant channel since the number of channels expressed can be increased sufficiently to allow accurate determinations of the pharmacological properties of this channel in the absence of Kv1.3. Fig. 4 panel A shows that the voltage-ramp applied evokes pure, non-voltage-gated hKCa3.1 currents, where the change in the slope of the current can be used to characterize the current block (Grissmer et al., 1993).

In addition to hKCa3.1, we assayed the effect of Vm24 on the currents of the following eight K^+ channels and a human cardiac Na^+ channel: mKv1.1 (Fig. 4B), hKv1.2 (Fig.4C), hKv1.4ΔN (fast inactivation removed hKv1.4, Fig. 4D), hKv1.5 (Fig. 4E), hKv2.1 (Fig. 4F), hKCa1.1 (BK, Fig. 4G), hKCa2.3 (SK, Fig. 4H), hKv11.1 (hERG, Fig. 4I), and hNav1.5 (Fig. 4J). Of the tested channels hKCa3.1, mKv1.1 and hKv1.2 were partially blocked by the peptide at 10 nM concentration while the other channels were unaffected (Figs. 4A-4J and 5A). This concentration is ~3500 times the K_d for hKv1.3 and resulted in RCF values of 0.59 ± 0.03, 0.80 ± 0.02 and 0.54 ± 0.08, for hKCa3.1, mKv1.1 and hKv1.2 channels, respectively (n=3 for each channel, Fig. 5A). The affected channels were further tested at 1 nM toxin concentration and yielded RCF values of 0.95±0.02, 0.97±0.02 and 0.81±0.02, respectively (Fig. 5B-5C; n=3 for

Molecular Pharmacology Fast Forward. Published on May 23, 2012 as DOI: 10.1124/mol.112.078006
This article has not been copyedited and formatted. The final version may differ from this version.

each channel). From the RCF values the affinity of Vm24 for these channels can be estimated from a model where 1 toxin molecule interacts with 1 channel to give K_d values between 14-30 nM for KCa3.1, 30-40 nM for mKv1.1 and 5-10 nM for hKv1.2. These values are at least 4500, 10000 and 1500 times higher than the K_d for Kv1.3, respectively.

Vm24 inhibits T cell proliferation, CD25 expression and Ca^{2+} signaling *in vitro* and suppresses DTH reaction *in vivo*.

High affinity and specific blockers of Kv1.3 channels inhibit distinctively the proliferation of human T cells (Hu et al., 2007). Accordingly, we assessed whether CD3/CD28-dependent T cell activation and proliferation was also inhibited by Vm24. Freshly isolated and proliferation-arrested human T lymphocytes were stimulated with the combination of anti-CD3 and anti-CD28 antibodies (cross-linked with polyclonal anti-mouse-IgG to maximize stimulation). The progression of the cell-cycle (i.e., the number of cell divisions) was followed using the CFSE dilution assay. Fig. 6A shows that preincubation of the cells with Vm24 prior to CD3×CD28 ligation resulted in a clear, dose-dependent reduction in the number of cells that proliferated after 96 hrs, yet it did not restrain the number of cell divisions of those cells that proliferated (Fig. 6A, left panels). Interestingly, the Vm24 concentrations that inhibited the proliferation are comparable to those that inhibited Kv1.3 channels in the electrophysiological assay, as shown by the overlap of the dose-response of the current block and the inhibition of the proliferation (Fig. 6B). Simultaneous addition of the peptide and the stimulus gave the same results (data not shown).

Upon T cell activation, the expression of the IL-2 receptor α-chain (CD25) is upregulated. Moreover, CD25 expression has been shown to parallel Kv1.3 activity, both in

Molecular Pharmacology Fast Forward. Published on May 23, 2012 as DOI: 10.1124/mol.112.078006
This article has not been copyedited and formatted. The final version may differ from this version.

CD4 and CD8 cells (Estes et al., 2008). Based on this, we tested whether Vm24 would interfere with the expression of CD25 in human T cells. Fig. 6A (right panels) show that addition of Vm24 30 minutes prior to T cell activation by CD3×CD28 ligation decreased the number of T lymphocytes expressing CD25 in a dose-dependent manner. Thus, the reduction in T cell proliferation observed in the presence of Vm24 was in part due to a reduction in the expression of CD25 (Fig. 6B).

As both T cell proliferation and CD25 expression depend on the Ca^{2+} signal accompanying T cell activation we tested the influence of Vm24 on the CD3×CD28 ligation-induced rise in the cytosolic free Ca^{2+} concentration ($[Ca^{2+}]_i$). T cells were incubated with Vm24 30 min before T cell activation and $[Ca^{2+}]_i$ was determined by microscopy. Fig. 6C shows that 10 nM Vm24 abrogated the CD3×CD28-dependent Ca^{2+} mobilization (Fig. 6C) yet it did not prevent the Ca^{2+} influx mediated by the calcium ionophore ionomycin. Together, these results suggest that the *in vitro* inhibition of proliferation and that of CD25 expression can be accounted for by the blocking of Kv1.3-mediated Ca^{2+} mobilization in human peripheral blood T lymphocytes.

We assessed the *in vivo* immunosuppressive capacity of Vm24 in by determining its potency to inhibit the active (Fig 7 A) or adoptive (Fig 7B) delayed type hypersensitivity (DTH) reaction. DTH is an example of a skin lesion caused by skin-homing T_{EM} cells (Soler et al., 2003). Active DTH reaction was evoked by ovalbumin immunization and a subsequent ovalbumin challenge, which results in the swelling of the challenged ear. Adoptive DTH was evoked by transferring *in vitro*-activated Ova-GFP T lymphocytes into the animals followed by an ovalbumin challenge. The treatment group of animals received a single dose of 0.1 mg/kg Vm24 subcutaneously at the time of the challenge, whereas control animals received a PBS

Molecular Pharmacology Fast Forward. Published on May 23, 2012 as DOI: 10.1124/mol.112.078006
This article has not been copyedited and formatted. The final version may differ from this version.

injection. The extent of the DTH reaction was evaluated 24 h later by measuring the specific ear swelling (Δ ear thickness), as described under Materials and Methods. Fig. 7 shows that a single dose of Vm24 significantly decreased the DTH response to ~35% or 65% of the treatment control, for active and adoptive DTH, respectively. This result is taken as a "proof-of-concept" that Vm24 works *in vivo* as an immunomodulatory agent.

Molecular Pharmacology Fast Forward. Published on May 23, 2012 as DOI: 10.1124/mol.112.078006
This article has not been copyedited and formatted. The final version may differ from this version.

DISCUSSION

We have characterized the *in vitro* pharmacological properties, and some *in vitro* and *in vivo* immunological effects of Vm24, a 36 amino acid-long peptide isolated from the venom of *Vaejovis mexicanus smithi*. Vm24 (α-KTx 23.1, (Gurrola et al., 2012)) is a high affinity blocker of Kv1.3 channels of human T cells, with an estimated K_d of 2.9 pM. The peptide exhibits at least 1500-fold selectivity for Kv1.3 over other ion channels tested. The application of picomolar concentrations of Vm24 inhibited the proliferation of normal human T lymphocytes *in vitro.* Vm24 also suppressed the DTH reaction in rats *in vivo,* which underscores the therapeutic potential of Vm24 as an immunosuppressive agent.

The mechanism by which scorpion toxins block K^+ channels is plugging the ion conduction pathway upon binding to the extracellular vestibule of the channel (Goldstein and Miller, 1993). We argue that Vm24 blocks Kv1.3 in a similar manner regardless of the slow and incomplete reversal of the current reduction: *i.*) the rate of current loss (at high toxin concentrations) depended on the concentration of Vm24, being faster at higher toxin concentrations; *ii.*) the leak current did not increase in the presence of the toxin, indicating the lack of the general damage of the membrane by Vm24; *iii.*) Vm24 did not inhibit several other K^+ currents or inhibited them quickly and reversibly (see below, in the selectivity profile of the toxin) which argues very strongly against a non-specific action of the toxin; *iv.*) simultaneous application of ChTx, a well-known pore blocker of Kv1.3, and Vm24 showed competition between the two toxins for the same binding site that was evident from the slowing of Vm24 blocking kinetics with increasing ChTx concentrations. Some of these arguments are discussed further below:

Molecular Pharmacology Fast Forward. Published on May 23, 2012 as DOI: 10.1124/mol.112.078006
This article has not been copyedited and formatted. The final version may differ from this version.

Ad *i.*) During the analysis of the blocking kinetics of the current (Fig. 1D) we estimated the molecular association rate constant, k_{on}, as the inverse of the time constant for the development of the block (i.e., $k_{on} \approx 1/\tau_{Vm24,in}$). This approach is valid for conditions where the dissociation rate of the toxin, k_{off} ($k_{off} = 1/\tau_{out}$, with $\tau_{out} \sim\sim 3800$ s, see Fig. 1C) is negligible as compared to $k_{on} \times [Vm24]$, the pseudo first-order association rate constant. This condition is fulfilled at [Vm24] where block of the Kv1.3 current developed within minutes. At higher [Vm24] (above 300 pM) the development of the block is too fast to be accurately resolved considering the minimum 15 s interval between successive current recordings (see Fig. 1B). The perfectly linear relationship between [Vm24] and $1/\tau_{Vm24,in}$ (in the concentration range of 10 pM and 300 pM) supports the validity of our approach (Fig. 1D). The $k_{on} = 9.55 \times 10^7$ $M^{-1}s^{-1}$ determined from this relationship is higher than typical values reported for peptide-channel interactions (Park and Miller, 1992b; Park and Miller, 1992a; Giangiacomo et al., 1993; Mullmann et al., 1999), but similar to the one determined for the ShK toxin (Middleton et al., 2003) and Pi2 (Peter et al., 2001) having picomolar affinities for Kv1.3.

Ad *iv.*) The strongest argument for a specific binding of Vm24 to the extracelluar vestibule is the competition between ChTx and Vm24 for the same, or overlapping binding sites on Kv1.3. This strategy was used to show mutually exclusive binding of tetraethylammonium and ChTx to the pore of Shaker K^+ channels (Goldstein and Miller, 1993). The strong linear dependence of $1/\tau_{in,Vm24}$ (see above) on the fraction of channels not blocked by ChTx ($r^2 = 0.967$) supports our conclusion for the mutually exclusive binding of Vm24 and ChTx to the pore of Kv1.3 (Fig. 2C).

The very slow onset and relief of the Kv1.3 current inhibition made it difficult to determine the extent of equilibrium by Vm24 and thus, it imposed limitations on the

Molecular Pharmacology Fast Forward. Published on May 23, 2012 as DOI: 10.1124/mol.112.078006
This article has not been copyedited and formatted. The final version may differ from this version.

determination of the equilibrium dissociation constant (K_d) (Fig. 3). Although the estimate of the k_{on} (Fig. 1D) is very high with $k_{on}=9.55\times10^7$ $M^{-1}s^{-1}$ the extremely low peptide concentrations make the pseudo-first order rate constant ($k_{on}\times$[Vm24]) very small. For example, at [Vm24]=3 pM, and considering the very slow off rate, the time-constant for reaching equilibrium block would be ~30 min. Thus, the slow wash-out kinetics and the possibility of the rundown of the peak currents lead to the use of an operational equilibrium block (see Materials and Methods) as the peak current where consecutive pulses in the presence of the toxin caused a negligible drop in the peak current (less than 2%). Thus, data presented in Fig. 3. represent upper limits for I/I_0 values, therefore, the K_d estimated from the dose-response relationship is also an overestimate of the real K_d. (Peter et al., 2001). The ratio of k_{off}/k_{on} returns K_d=2.75 pM which is in a good agreement with the one determined from the dose-response relationship. This indicates that the overestimation of the K_d from the dose-response was negligible, however, one should consider the assumptions used to obtain k_{on} and k_{off}. The slow onset of the block and the consequent inaccurate determination of the equilibrium block might have resulted in the significant discrepancy between the K_d values reported for the inhibition of Kv1.3 by ShK (Middleton et al., 2003).

Vm24 is similar to other *natural peptides* described in the literature regarding its high affinity blockade of the Kv1.3 channels. Among these peptides, the affinity of ShK (estimated IC_{50} = 0.9 pM (Middleton et al., 2003) or 11 pM (Kalman et al., 1998)), OSK-1 (α-KTx3.7, K_d=14 pM (Mouhat et al., 2005)), HgTx1 (α-KTx2.5, K_d=86 pM, (Koschak et al., 1998)), MgTx (α-KTx2.2, K_d= 50 pM, (Garcia-Calvo et al., 1993)) and that of HsTx1 (α-KTx6.3, K_d=12 pM (Lebrun et al., 1997)) for Kv1.3 are remarkable. However, these peptides are all less selective for Kv1.3 than Vm24; some of these have similar or even higher affinity for Kv1.1 than Kv1.3

Molecular Pharmacology Fast Forward. Published on May 23, 2012 as DOI: 10.1124/mol.112.078006
This article has not been copyedited and formatted. The final version may differ from this version.

(ShK and HgTx1 and MgTx1) while others are selective for Kv1.3, but to a lower extent than Vm24 (43 to 636-fold for OSK-1 and HsTx1, respectively) On the contrary, the selectivity of Vm24 over other ion channels tested is at least 1500-fold based on the K_d value obtained from the dose-response relationship and the single-concentration estimates of the K_d values for those channels which were inhibited by Vm24. This value is well over the commonly accepted criteria for selectivity, which is defined as 100-fold difference in the equilibrium dissociation constant for an α-KTx binding to two different potassium channels (Giangiacomo et al., 2004). The ion channels which were inhibited at 10 nM [Vm24] were Kv1.1, Kv1.2 and KCa3.1, whereas other tested channels are practically resistant to Vm24. Of note, 10 nM [Vm24] is more than 3000-fold higher concentration than the overestimated K_d for Kv1.3. Data presented in Fig. 5 indicate that the order of blocking potency of Vm24 for various ion channels is hKv1.3 >>> hKv1.2 > hKCa3.1 > mKv1.1 >>> hKv1.4 ≈ hKv1.5 ≈ rKv2.1 ≈ hKv11.1 ≈ hKCa1.1 ≈ hKCa2.3 ≈ $hNa_V1.5$. The >1500-fold selectivity of Vm24 is significantly better than the Kv1.3 selectivity achieved for recombinant mutant peptide toxins such as various OSK1 mutants (e.g. [K16,D20]-OSK1 (Mouhat et al., 2005)), [R11,T28,H33]-BmKTx (Han et al., 2008) and ShK(L192) (Pennington et al., 2009) for which toxins selectivity ranged between 9 to 340-fold.

Key features of high affinity Kv1.3 inhibitors are that they interfere with T cell receptor activation-induced Ca^{2+} signaling and the subsequent cell proliferation (Cahalan and Chandy, 2009). These characteristic features are clearly demonstrated for Vm24 in this paper. Vm24, in concentrations overlapping with the block of the Kv1.3 current, inhibited the anti CD3×CD28-iduced T cell proliferation and the expression of the high affinity interleukin-2 receptor α. Since Kv1.3 is the dominant K^+ channel of resting T cells of either subset (i.e., naïve or T_{EM}) their proliferation is sensitive to Kv1.3 inhibition (Wulff et al., 2003). However, the inhibition of the

Molecular Pharmacology Fast Forward. Published on May 23, 2012 as DOI: 10.1124/mol.112.078006
This article has not been copyedited and formatted. The final version may differ from this version.

proliferation is not complete, as in case of Vm24 also, even at peptide concentrations which fully inhibit Kv1.3 (Wulff et al., 2003; Hu et al., 2007). This may be an indication of the presence of other, recently described K^+ channel types in these cells (Meuth et al., 2008). A more appropriate and widely used Kv1.3-inhibition specific immunological test is the inhibition of DTH in rats (Beeton et al., 2006). The proliferation of T_{EM} cells responsible for DTH is persistently inhibited by highly selective Kv1.3 inhibitors, resulting in a decreased DTH response. The potency of Vm24 to reduce DTH is similar to that of other peptides (e.g. ShK 192, (Pennington et al., 2009)), a single dose of 0.1 mg/kg Vm24 efficiently inhibited both active and adoptive DTH. Thus, in general, the biological activity of Vm24 *in vitro* at cellular level (proliferation, Ca^{2+} signal) as well as *in vivo* resembles that of other high affinity and high selectivity Kv1.3 inhibitors.

The unique primary structure and the extremely high affinity and selectivity of Vm24 for Kv1.3 make this natural peptide an ideal tool to suppress T_{EM}-dependent immunological reactions *in vivo* without significant side effects of general immunosuppression. This confers a therapeutic potential to Vm24 in T_{EM}-dependent human autoimmune diseases such as MS, rheumatoid arthritis and psoriasis.

ACKNOWLEDGEMENTS: The authors thank Cecilia Nagy and Erika Melchy for technical support.

AUTHORSHIP CONTRIBUTIONS:

Participated in research design: Possani, Panyi, Beeton, Rosenstein, Rodríguez de la Vega, Gurrola-Briones, Gaspar.

Conducted experiments: Gurrola-Briones, Pedraza-Alva, Varga, Cardenas, Tajhya, Papp.

Contributed new reagents or analytic tools:.

Performed data analysis: Possani, Panyi, Beeton, Varga, Rosenstein, Gurrola-Briones, Pedraza-Alva, Gaspar, Cardenas, Tajhya, Papp.

Wrote or contributed to the writing of the manuscript: Possani, Panyi, Varga, Beeton, Rosenstein, Rodríguez de la Vega.

REFERENCES

Avdonin V, Tang XD and Hoshi T (2003) Stimulatory Action of Internal Protons on Slo1 BK Channels. *Biophys J* **84**:2969-2980.

Bagdany M, Batista CV, Valdez-Cruz NA, Somodi S, Rodriguez de la Vega RC, Licea AF, Varga Z, Gaspar R, Possani LD and Panyi G (2005) Anuroctoxin, a New Scorpion Toxin of the Alpha-KTx 6 Subfamily, Is Highly Selective for Kv1.3 Over IKCa1 Ion Channels of Human T Lymphocytes. *Mol Pharmacol* **67**:1034-1044.

Batista CV, Roman-Gonzalez SA, Salas-Castillo SP, Zamudio FZ, Gomez-Lagunas F and Possani LD (2007) Proteomic Analysis of the Venom From the Scorpion Tityus Stigmurus: Biochemical and Physiological Comparison With Other Tityus Species. *Comp Biochem Physiol C Toxicol Pharmacol* **146**:147-157.

Beeton C and Chandy KG (2007a) Induction and Monitoring of Active Delayed Type Hypersensitivity (DTH) in Rats. *J Vis Exp* **6**.

Beeton C and Chandy KG (2007b) Induction and Monitoring of Adoptive Delayed Type Hypersensitivity in Rats. *J Vis Exp* **8**.

Beeton C, Wulff H, Standifer NE, Azam P, Mullen KM, Pennington MW, Kolski-Andreaco A, Wei E, Grino A, Counts DR, Wang PH, Leehealey CJ, Andrews S, Sankaranarayanan A, Homerick D, Roeck WW, Tehranzadeh J, Stanhope KL, Zimin P, Havel PJ, Griffey S, Knaus HG, Nepom GT, Gutman GA, Calabresi PA and Chandy KG (2006) Kv1.3 Channels Are a Therapeutic Target for T Cell-Mediated Autoimmune Diseases. *Proc Natl Acad Sci U S A* **103**:17414-17419.

Cahalan MD and Chandy KG (2009) The Functional Network of Ion Channels in T Lymphocytes. *Immunol Rev* **231**:59-87.

Corzo G, Papp F, Varga Z, Barraza O, Espino-Solis PG, Rodriguez de la Vega RC, Gaspar R, Panyi G and Possani LD (2008) A Selective Blocker of Kv1.2 and Kv1.3 Potassium Channels From the Venom of the Scorpion Centruroides Suffusus Suffusus. *Biochem Pharmacol* **76**:1142-1154.

Dauplais M, Lecoq A, Song J, Cotton J, Jamin N, Gilquin B, Roumestand C, Vita C, de Medeiros CL, Rowan EG, Harvey AL and Menez A (1997) On the Convergent Evolution of Animal Toxins. Conservation of a Diad of Functional Residues in Potassium Channel-Blocking Toxins With Unrelated Structures. *J Biol Chem* **272**:4302-4309.

Estes DJ, Memarsadeghi S, Lundy SK, Marti F, Mikol DD, Fox DA and Mayer M (2008) High-Throughput Profiling of Ion Channel Activity in Primary Human Lymphocytes. *Anal Chem* **80**:3728-3735.

Fierro NA, Pedraza-Alva G and Rosenstein Y (2006) TCR-Dependent Cell Response Is Modulated by the Timing of CD43 Engagement. *J Immunol* **176**:7346-7353.

Garcia-Calvo M, Leonard RJ, Novick J, Stevens SP, Schmalhofer W, Kaczorowski GJ and Garcia ML (1993) Purification, Characterization, and Biosynthesis of Margatoxin, a Component of Centruroides Margaritatus Venom That Selectively Inhibits Voltage-Dependent Potassium Channels. *J Biol Chem* **268**:18866-18874.

Ghanshani S, Wulff H, Miller MJ, Rohm H, Neben A, Gutman GA, Cahalan MD and Chandy KG (2000) Up-Regulation of the IKCa1 Potassium Channel During T-Cell Activation. Molecular Mechanism and Functional Consequences. *J Biol Chem* **275**:37137-37149.

Giangiacomo KM, Ceralde Y and Mullmann TJ (2004) Molecular Basis of Alpha-KTx Specificity. *Toxicon* **43**:877-886.

Giangiacomo KM, Sugg EE, Garcia-Calvo M, Leonard RJ, McManus OB, Kaczorowski GJ and Garcia ML (1993) Synthetic Charybdotoxin-Iberiotoxin Chimeric Peptides Define Toxin Binding Sites on Calcium-Activated and Voltage-Dependent Potassium Channels. *Biochemistry* **32**:2363-2370.

Goldstein SA and Miller C (1993) Mechanism of Charybdotoxin Block of a Voltage-Gated K^+ Channel. *Biophys J* **65**:1613-1619.

Grissmer S, Nguyen AN, Aiyar J, Hanson DC, Mather RJ, Gutman GA, Karmilowicz MJ, Auperin DD and Chandy KG (1994) Pharmacological Characterization of Five Cloned Voltage-Gated K^+ Channels, Types Kv1.1, 1.2, 1.3, 1.5, and 3.1, Stably Expressed in Mammalian Cell Lines. *Mol Pharmacol* **45**:1227-1234.

Grissmer S, Nguyen AN and Cahalan MD (1993) Calcium-Activated Potassium Channels in Resting and Activated Human T Lymphocytes. Expression Levels, Calcium Dependence, Ion Selectivity, and Pharmacology. *J Gen Physiol* **102**:601-630.

Gurrola GB, Hernández-López RA, Rodríguez de la Vega RC, Varga Z, Batista CV, Salas-Castillo SP, Panyi G, Del Río-Portilla F, Possani LD (2012) Structure, Function, and Chemical Synthesis of Vaejovis mexicanus Peptide 24: A Novel Potent Blocker of Kv1.3 Potassium Channels of Human T Lymphocytes. *Biochemistry* **51**:4049-4061.

Han S, Yi H, Yin SJ, Chen ZY, Liu H, Cao ZJ, Wu YL and Li WX (2008) Structural Basis of a Potent Peptide Inhibitor Designed for Kv1.3 Channel, a Therapeutic Target of Autoimmune Disease. *J Biol Chem* **283**:19058-19065.

Hu L, Pennington M, Jiang Q, Whartenby KA and Calabresi PA (2007) Characterization of the Functional Properties of the Voltage-Gated Potassium Channel Kv1.3 in Human $CD4^+$ T Lymphocytes. *J Immunol* **179**:4563-4570.

Kalman K, Pennington MW, Lanigan MD, Nguyen A, Rauer H, Mahnir V, Paschetto K, Kem WR, Grissmer S, Gutman GA, Christian EP, Cahalan MD, Norton RS and Chandy KG (1998)

ShK-Dap22, a Potent Kv1.3-Specific Immunosuppressive Polypeptide. *J Biol Chem* **273**:32697-32707.

Koch RO, Wanner SG, Koschak A, Hanner M, Schwarzer C, Kaczorowski GJ, Slaughter RS, Garcia ML and Knaus HG (1997) Complex Subunit Assembly of Neuronal Voltage-Gated K^+ Channels. Basis for High-Affinity Toxin Interactions and Pharmacology. *J Biol Chem* **272**:27577-27581.

Koschak A, Bugianesi RM, Mitterdorfer J, Kaczorowski GJ, Garcia ML and Knaus HG (1998) Subunit Composition of Brain Voltage-Gated Potassium Channels Determined by Hongotoxin-1, a Novel Peptide Derived From Centruroides Limbatus Venom. *J Biol Chem* **273**:2639-2644.

Lebrun B, Romi-Lebrun R, Martin-Eauclaire MF, Yasuda A, Ishiguro M, Oyama Y, Pongs O and Nakajima T (1997) A Four-Disulphide-Bridged Toxin, With High Affinity Towards Voltage-Gated K^+ Channels, Isolated From Heterometrus Spinnifer (Scorpionidae) Venom. *Biochem J* **328 (Pt 1)**:321-327.

Leonard RJ, Garcia ML, Slaughter RS and Reuben JP (1992) Selective Blockers of Voltage-Gated K^+ Channels Depolarize Human T Lymphocytes: Mechanism of the Antiproliferative Effect of Charybdotoxin. *Proc Natl Acad Sci U S A* **89**:10094-10098.

Lewis RS (2001) Calcium Signaling Mechanisms in T Lymphocytes. *Annu Rev Immunol* **19**:497-521.

Lin CS, Boltz RC, Blake JT, Nguyen M, Talento A, Fischer PA, Springer MS, Sigal NH, Slaughter RS, Garcia ML, Kaczorowski GJ and Koo GC (1993) Voltage-Gated Potassium Channels Regulate Calcium-Dependent Pathways Involved in Human T Lymphocye Activation. *J Exp Med* **177**:637-645.

Matteson DR and Deutsch C (1984) K Channels in T Lymphocytes: a Patch Clamp Study Using Monoclonal Antibody Adhesion. *Nature* **307**:468-471.

Meuth SG, Bittner S, Meuth P, Simon OJ, Budde T and Wiendl H (2008) TWIK-Related Acid-Sensitive K^+ Channel 1 (TASK1) and TASK3 Critically Influence T Lymphocyte Effector Functions. *J Biol Chem* **283**:14559-14570.

Middleton RE, Sanchez M, Linde AR, Bugianesi RM, Dai G, Felix JP, Koprak SL, Staruch MJ, Bruguera M, Cox R, Ghosh A, Hwang J, Jones S, Kohler M, Slaughter RS, McManus OB, Kaczorowski GJ and Garcia ML (2003) Substitution of a Single Residue in Stichodactyla Helianthus Peptide, ShK-Dap22, Reveals a Novel Pharmacological Profile. *Biochemistry* **42**:13698-13707.

Mouhat S, Visan V, Ananthakrishnan S, Wulff H, Andreotti N, Grissmer S, Darbon H, De Waard M and Sabatier JM (2005) K^+ Channel Types Targeted by Synthetic OSK1, a Toxin From Orthochirus Scrobiculosus Scorpion Venom. *Biochemical Journal* **385**:95-104.

Mullmann TJ, Munujos P, Garcia ML and Giangiacomo KM (1999) Electrostatic Mutations in Iberiotoxin As a Unique Tool for Probing the Electrostatic Structure of the Maxi-K Channel Outer Vestibule. *Biochemistry* **38**:2395-2402.

Muul LM, Silvin C, James SP and Candotti F (2008) Measurement of Proliferative Responses of Cultured Lymphocytes. *Curr Protoc Immunol* **Chapter 7**:Unit-7.

Panyi G, Possani LD, Rodriguez de la Vega RC, Gaspar R and Varga Z (2006) K^+ Channel Blockers: Novel Tools to Inhibit T Cell Activation Leading to Specific Immunosuppression. *Curr Pharm Des* **12**:2199-2220.

Panyi G, Varga Z and Gaspar R (2004) Ion Channels and Lymphocyte Activation. *Immunol Lett* **92**:55-66.

Park CS and Miller C (1992a) Interaction of Charybdotoxin With Permeant Ions Inside the Pore of a K^+ Channel. *Neuron* **9**:307-313.

Park CS and Miller C (1992b) Mapping Function to Structure in a Channel-Blocking Peptide: Electrostatic Mutants of Charybdotoxin. *Biochemistry* **31**:7749-7755.

Pennington MW, Beeton C, Galea CA, Smith BJ, Chi V, Monaghan KP, Garcia A, Rangaraju S, Giuffrida A, Plank D, Crossley G, Nugent D, Khaytin I, Lefievre Y, Peshenko I, Dixon C, Chauhan S, Orzel A, Inoue T, Hu X, Moore RV, Norton RS and Chandy KG (2009) Engineering a Stable and Selective Peptide Blocker of the Kv1.3 Channel in T Lymphocytes. *Mol Pharmacol* **75**:762-773.

Peter MJ, Varga Z, Hajdu P, Gaspar RJ, Damjanovich S, Horjales E, Possani LD and Panyi G (2001) Effects of Toxins Pi2 and Pi3 on Human T Lymphocyte Kv1.3 Channels: the Role of Glu7 and Lys24. *J Membr Biol* **179**:13-25.

Soler D, Humphreys TL, Spinola SM and Campbell JJ (2003) CCR4 Versus CCR10 in Human Cutaneous TH Lymphocyte Trafficking. *Blood* **101**:1677-1682.

Wulff H, Calabresi PA, Allie R, Yun S, Pennington M, Beeton C and Chandy KG (2003) The Voltage-Gated Kv1.3 K^+ Channel in Effector Memory T Cells As New Target for MS. *J Clin Invest* **111**:1703-1713.

Wulff H, Gutman GA, Cahalan MD and Chandy KG (2001) Delineation of the Clotrimazole/TRAM-34 Binding Site on the Intermediate Conductance Calcium-Activated Potassium Channel, IKCa1. *J Biol Chem* **276**:32040-32045.

Molecular Pharmacology Fast Forward. Published on May 23, 2012 as DOI: 10.1124/mol.112.078006
This article has not been copyedited and formatted. The final version may differ from this version.

FOOTNOTES

This work was supported by OTKA [K 60740, NK 61412]; Tásadalmi Megújulás Operatív Program [TÁMOP 4.2.2-08/1/2008-0019, TÁMOP-4.2.1/B-09/1/KONV-2010-007, TÁMOP 4.2.2-A-11/1/KONV-2012-0025], DGAPA-UNAM [IN204110]; CONACyT-Mexico and TéT Hungary [MX-10/207]; NINDS [NS073712]. RCRV receives funding from the European Union Seventh Framework Programme FP7/2007-2013 [Grant Number 246556]. Z.V. is a Bolyai Fellow.

Molecular Pharmacology Fast Forward. Published on May 23, 2012 as DOI: 10.1124/mol.112.078006
This article has not been copyedited and formatted. The final version may differ from this version.

LEGENDS FOR FIGURES

Fig. 1 Block of Kv1.3 channels by Vm24. A) Whole-cell potassium currents through hKv1.3 channels were evoked from a human T cell in response to depolarizing pulses to +50 mV from a holding potential of -120 mV every 15s. Currents in the absence of Vm24 (control, indicated by arrow) are almost completely blocked when 1 nM Vm24 is administered to the cell via the perfusion of the extracellular medium. Arrows indicate the 1^{st} and the 12^{th} pulses in Vm24. B) The normalized peak currents as a function of time are shown following the application of 1 nM (filled circles) or 0.3 nM (empty circles) of Vm24. Arrow indicates the start of the application of the toxin. C) The normalized peak currents of a lymphocyte as a function of time are shown as 3 pM Vm24 is applied to the cell and then removed (wash-out) from the extracellular medium. Perfusion with a toxin-free medium resulted in a very slow partial recovery from block with a time constant of ~3800 s. Pulses were delivered every 30s. D) The rate of block (inverse of the wash-in time constant, $\tau_{Vm24,in}$) as a function of the Vm24 concentration. Data points were fitted with a linear function, $r^2 = 0.99$.

Fig. 2: Competition between ChTx and Vm24. A) Peak whole-cell Kv1.3 currents of a human T cell sequentially exposed to 0.3 nM ChTx, and after the equilibration of the block, to a mixture of 0.3 nM ChTx and 0.3 nM Vm24 are shown as indicated by the arrows. Block kinetics by Vm24 was measured by fitting the peak currents with a decaying single exponential and determining the time constant. B) Normalized peak currents of human T cells illustrate the block kinetics by 0.3 nM Vm24 in the absence and in the presence of the indicated concentrations ChTx. C) The rate of block (inverse of the wash-in time constant) by 0.3 nM Vm24 as a function

Molecular Pharmacology Fast Forward. Published on May 23, 2012 as DOI: 10.1124/mol.112.078006
This article has not been copyedited and formatted. The final version may differ from this version.

of the remaining current fraction (unblocked channel fraction) in the absence and presence of 0.3, 1 or 2.5 nM ChTx is shown. Data points were fitted with a linear function, $r^2 = 0.967$.

Fig. 3: The dose-response relationship for Vm24 was obtained by plotting the remaining current fraction (RCF=I / I_0) as a function of toxin concentration, where I and I_0 are the peak currents measured in the presence and absence of the toxin, respectively, and fitting the data points with the function: $RCF = K_d^n / (K_d^n + [Tx]^n)$, where [Tx] indicates the toxin concentration and K_d is the dissociation constant. Error bars indicate SEM (n = 3–6). The dose-response function constructed this way yields a K_d = 2.9 pM and a Hill coefficient n~1. For the determination of the equilibrium block, see Materials and Methods

Fig. 4: Vm24 has little or no effect on several ion channels. Current traces recorded before the application of the toxin (control), following the equilibration of block by 10 nM Vm24 and following wash-out (wash) of the toxin are shown as indicated by the arrows for the following channels: A) hKCa3.1 (or hIKCa1, Ca^{2+} activated K^+ channels of T lymphocytes); B) mKv1.1; C) hKv1.2; D) fast inactivation-removed hKv1.4 (Kv1.4ΔN); E) hKv1.5; F) rKv2.1; G) KCa1.1 (hBK); H) hKCa2.3 (hSK); I) hKv11.1 (hERG; J) Nav1.5. For the expression systems, solutions and voltage protocols see Materials and Methods.

Fig. 5: Vm 24 is selective for Kv1.3 channels. A) Bars indicate the remaining current fractions at equilibrium block of the indicated channels by Vm24 applied at 10 nM concentration. Data is presented as mean ± SEM, for n≥3 independent experiments. B) Channels that were partially blocked by 10 nM toxin were tested again at 1 nM Vm24 and the remaining current fractions are

shown by the bars. C) Effect of 1 nM Vm24 on Kv1.1, Kv1.2 and KCa3.1 currents. Current traces recorded before the application of the toxin (control), following the equilibration of block by 1 nM Vm24 and following wash-out (wash) of the toxin are shown as indicated by the arrows. For the expression systems, solutions and voltage protocols see Materials and Methods.

Fig. 6: In *vitro* effects of Vm24 on T cell functions. A) (left panel) CD3-CD28 induced proliferation is inhibited in the presence of Vm24. Resting human T lymphocytes were activated by crosslinking CD3 and CD28, in the absence (Control) or presence of the indicated dose of Vm24. Cell proliferation was evaluated after 96 h by CFSE dilution, (right panel) Vm24 controls CD25 expression. Purified resting human CD4 lymphocytes were activated by CD3 and CD28 engagement in the presence or absence (Control) of different doses of Vm24 and, following 24 h stimulation, the level of CD25 expression on the cell surface was measured by flow cytometry. Results are representative of at least three independent experiments. B) Overlap between the dose-responses of the current inhibition (1−RCF) and the inhibition of proliferation and CD25 expression. Triangles, squares and circles indicate the inhibition of Kv1.3 current, the CD25 expression, and the inhibition of proliferation, respectively, as a function of Vm24 concentration. C) Vm24 prevents CD3×CD28 dependent Ca^{2+} mobilization. Fura-2 ratios are shown for representative T cells. The calcium response of human peripheral blood T cells to CD3 and CD28 engagement was evaluated using anti-CD3 and anti-CD38 antibodies and rabbit anti-mouse IgGs (RaMIG) in a crosslinking system, in the absence (Control) or presence 10 nM Vm24. At the end of the experiment the calcium ionophore inomycin was applied (arrow) as a positive control. Results are representative of at least three independent experiments.

Molecular Pharmacology Fast Forward. Published on May 23, 2012 as DOI: 10.1124/mol.112.078006
This article has not been copyedited and formatted. The final version may differ from this version.

Fig. 7: Vm24 inhibits DTH reaction in rats. Data are shown as difference in ear thickness between the ovalbumin-challenged left ear and the saline-injected right ear (mean ± SEM). The treatment group of animals (solid bars) received a single dose of 0.1 mg/kg Vm24 subcutaneously at the time of the challenge whereas the control group received the vehicle (PBS+2% rat serum, open pars). **(a)** Vm24 inhibits active DTH directed against ovalbumin. N = 7 rats per group. $^{**}p \leq 0.01$. **(b)** Vm24 inhibits adoptive DTH induced with $Kv1.3^{high}$ activated Ova-GFP T lymphocytes. N = 9 rats per group. $^{*}p \leq 0.05$.

Molecular Pharmacology Fast Forward. Published on May 23, 2012 as DOI: 10.1124/mol.112.078006
This article has not been copyedited and formatted. The final version may differ from this version.

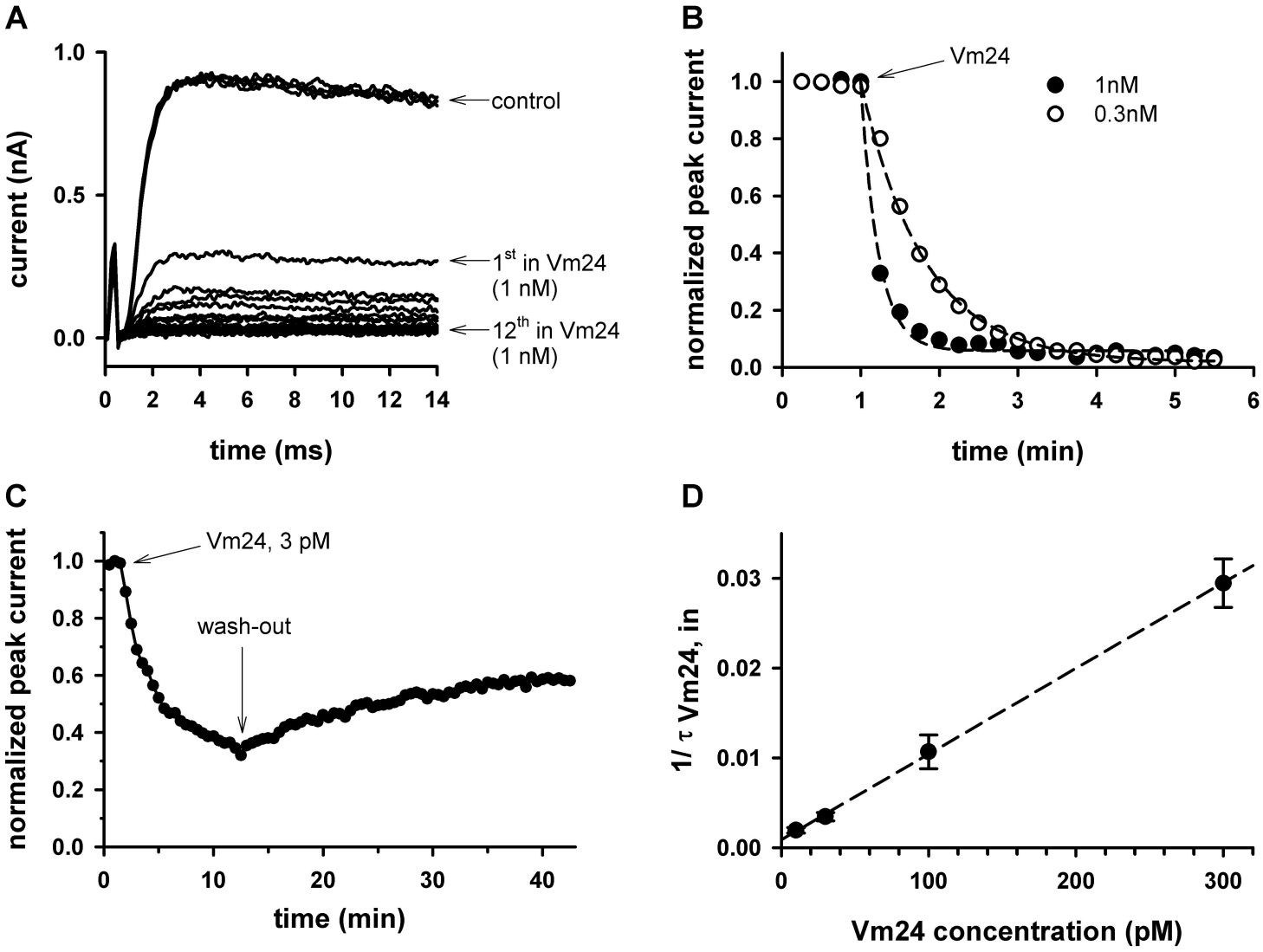

Fig. 1

Molecular Pharmacology Fast Forward. Published on May 23, 2012 as DOI: 10.1124/mol.112.078006
This article has not been copyedited and formatted. The final version may differ from this version.

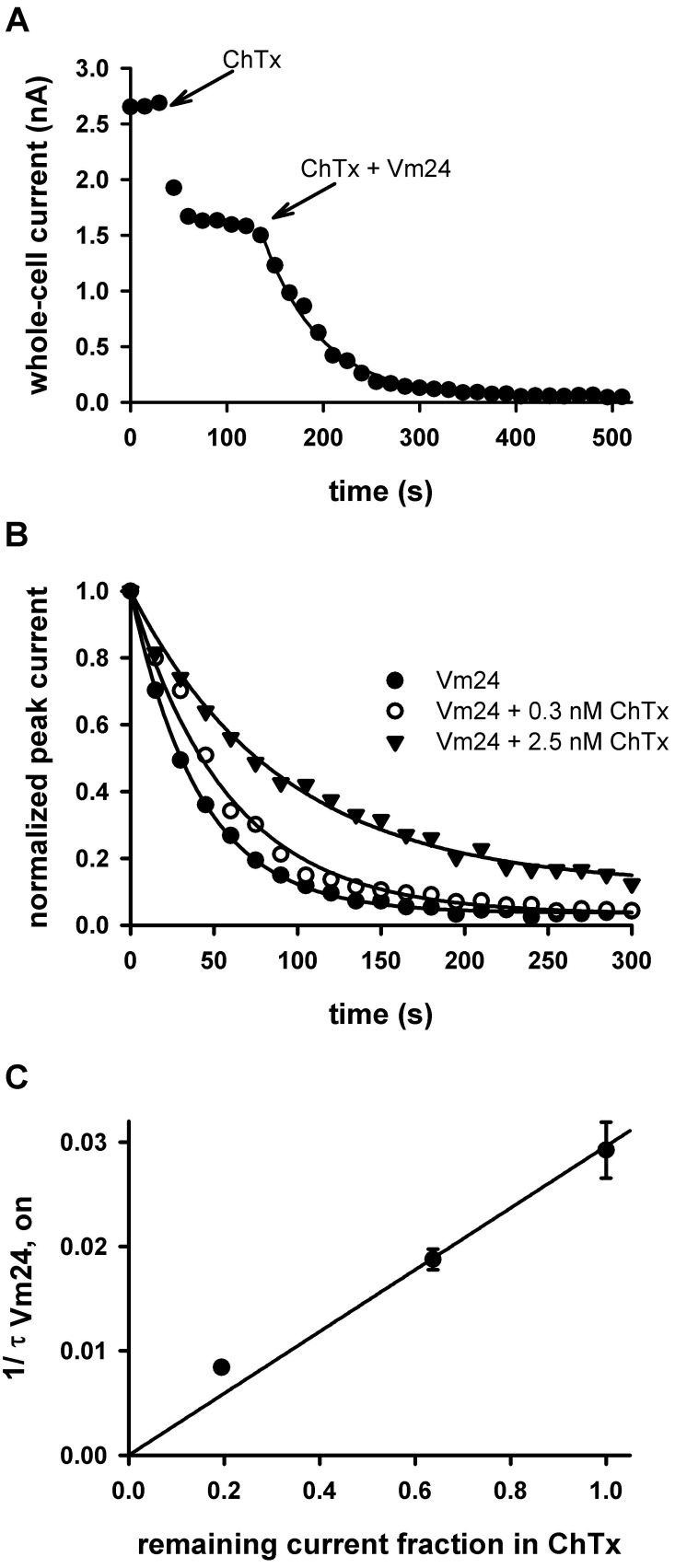

Fig. 2

Molecular Pharmacology Fast Forward. Published on May 23, 2012 as DOI: 10.1124/mol.112.078006
This article has not been copyedited and formatted. The final version may differ from this version.

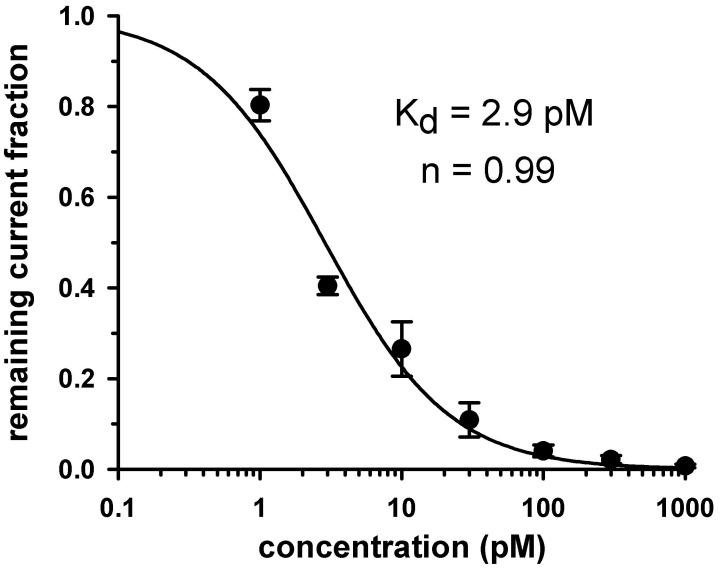

Fig. 3.

Molecular Pharmacology Fast Forward. Published on May 23, 2012 as DOI: 10.1124/mol.112.078006
This article has not been copyedited and formatted. The final version may differ from this version.

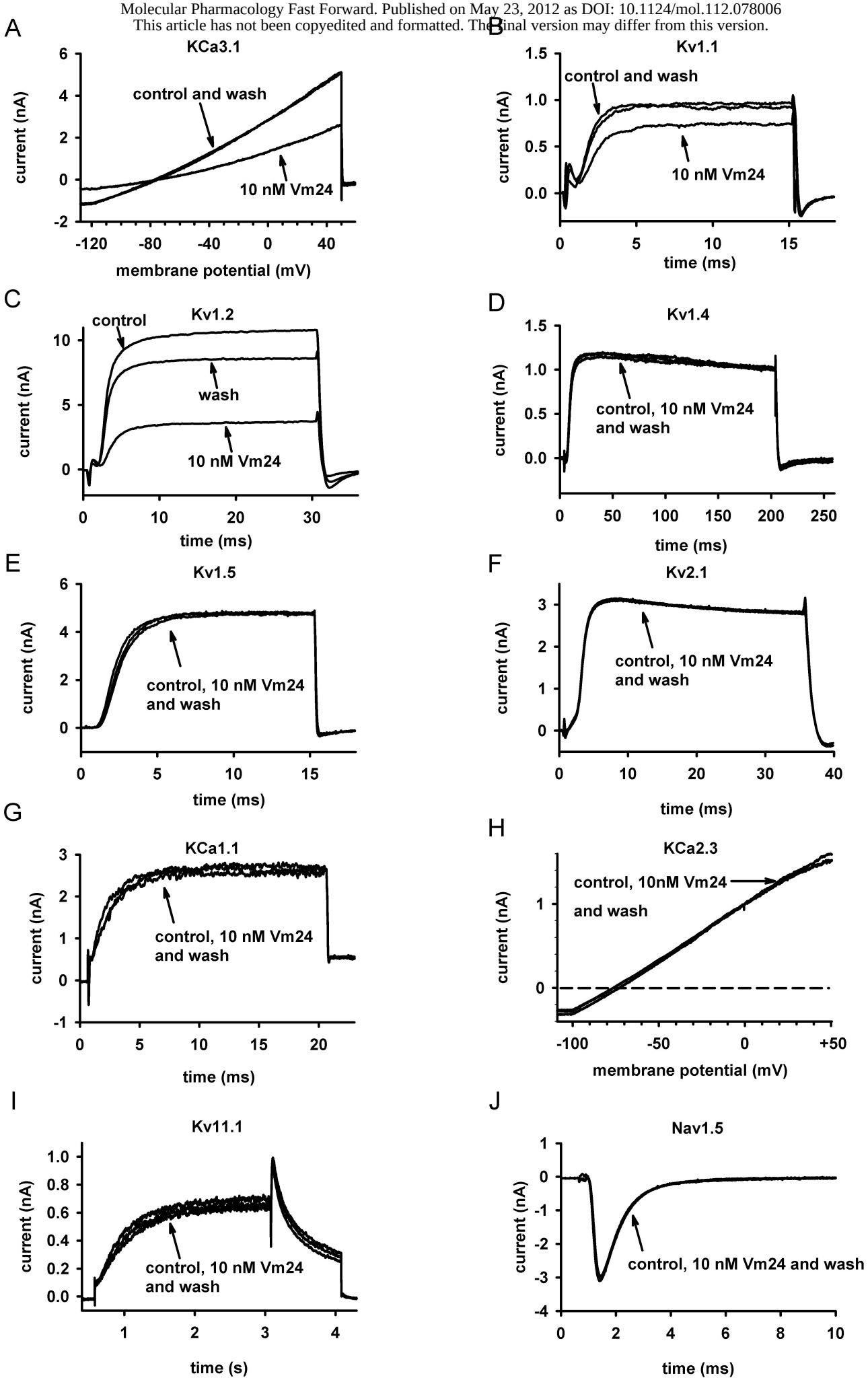

Fig. 4.

Molecular Pharmacology Fast Forward. Published on May 23, 2012 as DOI: 10.1124/mol.112.078006
This article has not been copyedited and formatted. The final version may differ from this version.

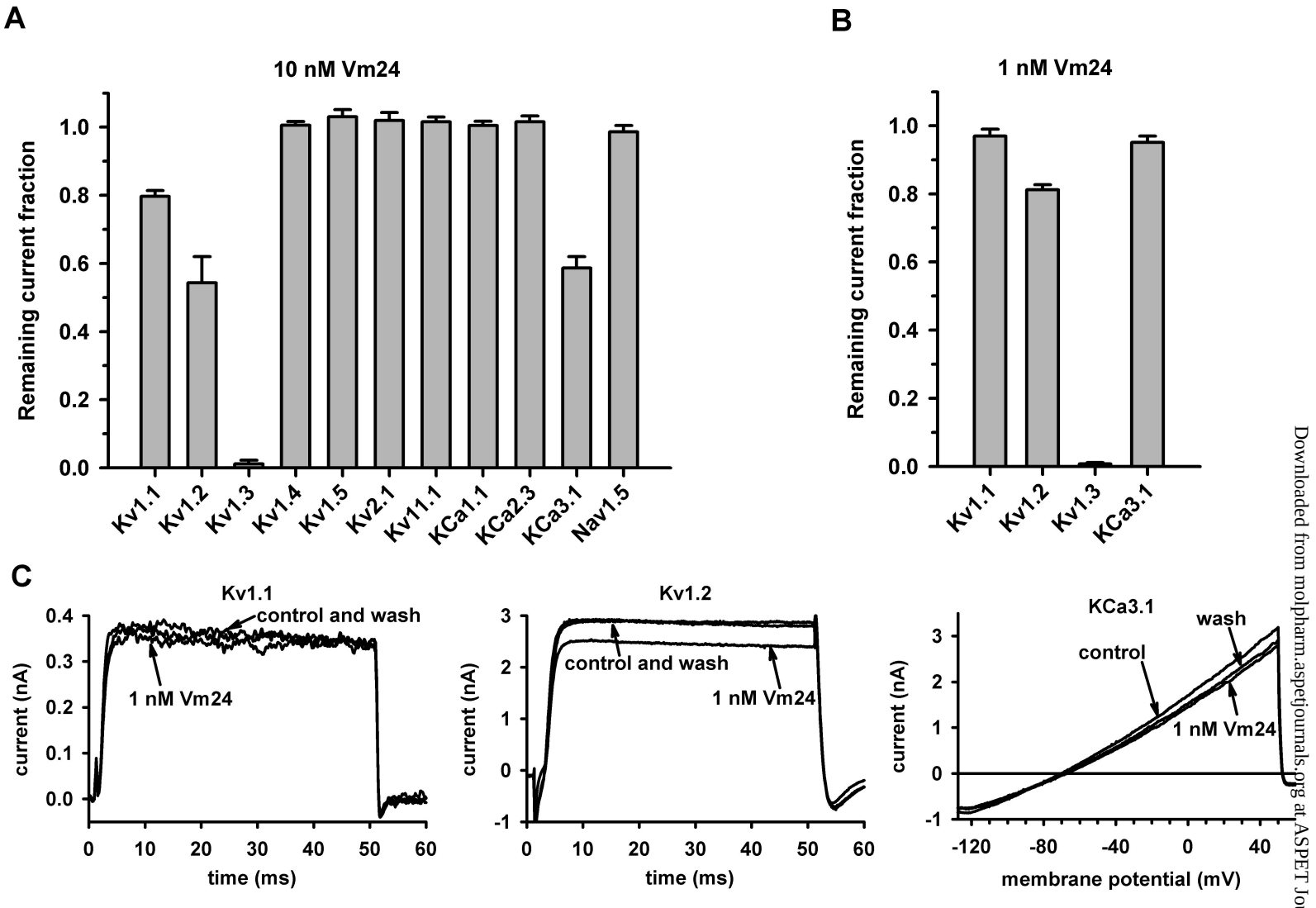

Fig. 5

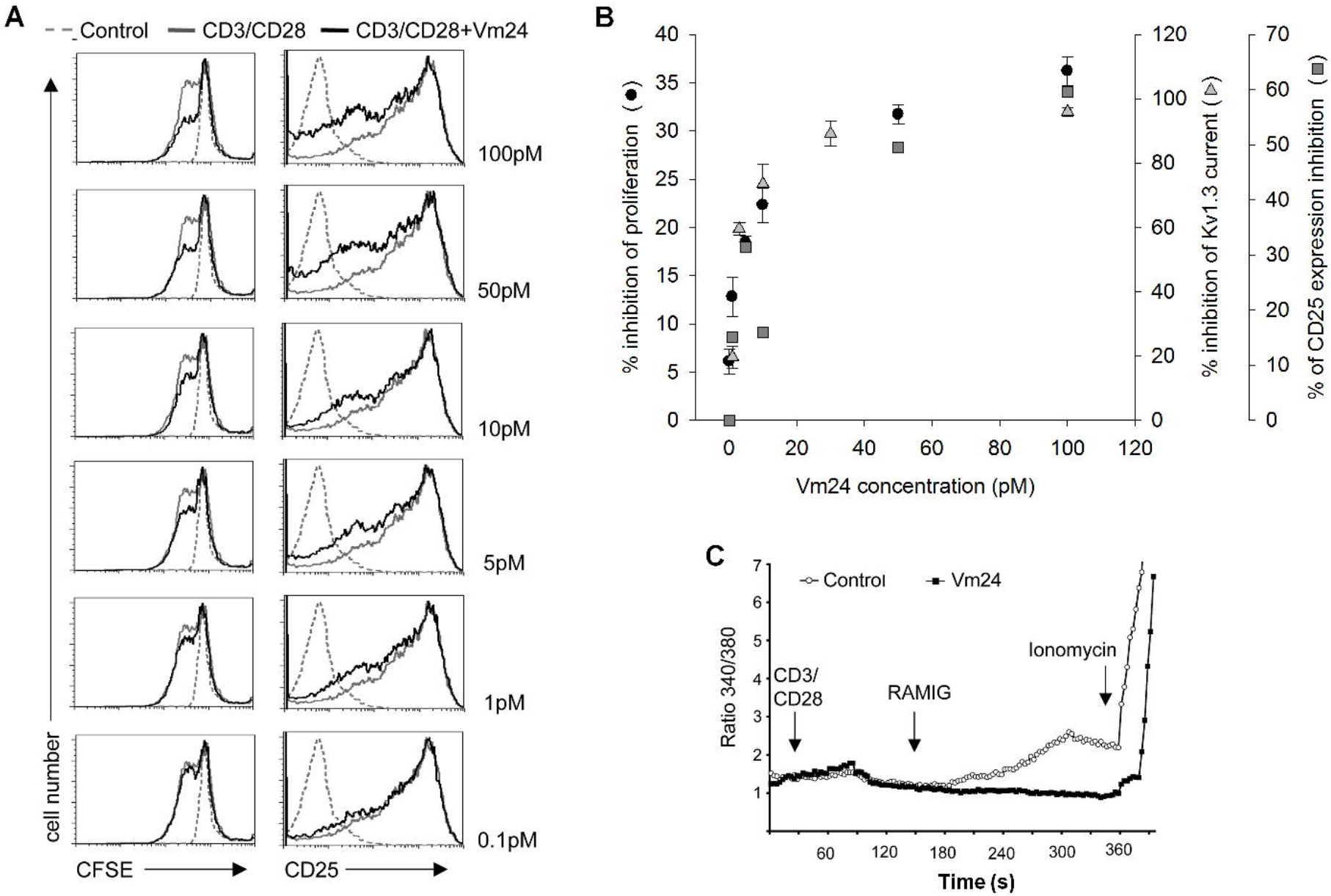
A
Control
CD3/CD28
CD3/CD28+Vm24
100pM
50pM
10pM
5pM
1pM
0.1pM
cell number
CFSE
CD25
B
% inhibition of proliferation (●)
% inhibition of Kv1.3 current (△)
% of CD25 expression inhibition (■)
Vm24 concentration (pM)
C
Control
Vm24
Ratio 340/380
CD3/
CD28
RAMIG
Ionomycin
Time (s)

Fig. 6

Molecular Pharmacology Fast Forward. Published on May 23, 2012 as DOI: 10.1124/mol.112.078006
This article has not been copyedited and formatted. The final version may differ from this version.

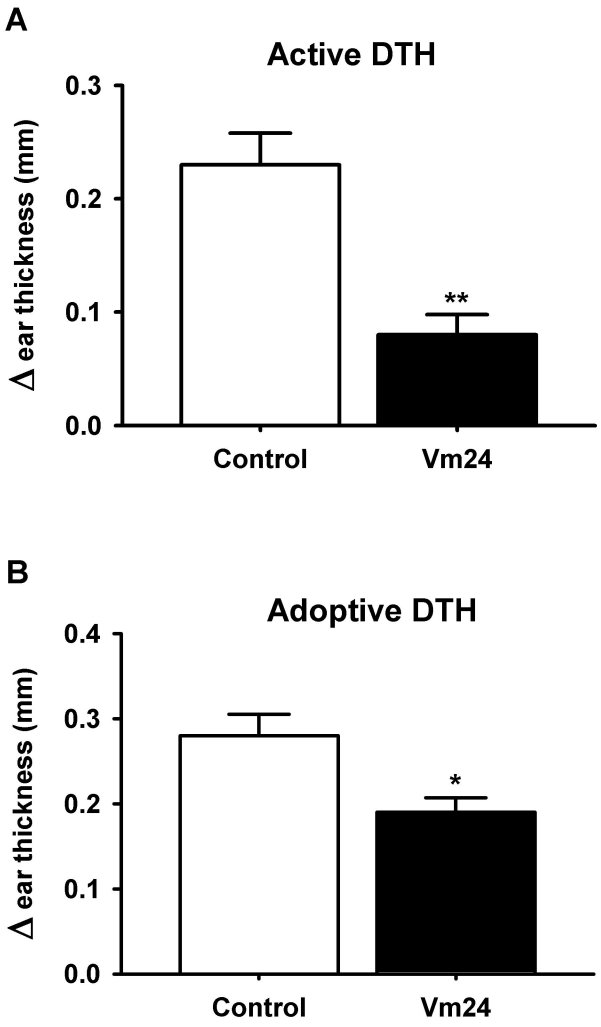

Fig. 7